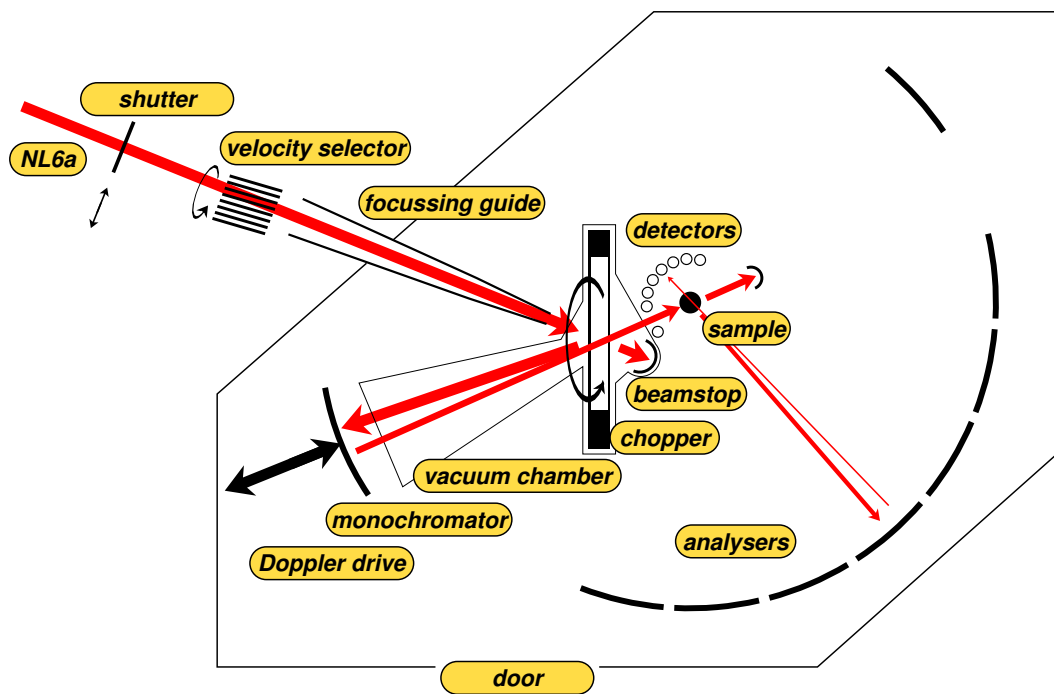


SPHERES

Backscattering spectrometer

J. Wuttke



Contents

1	Introduction	3
2	Spectrometer Physics	3
2.1	Energy Selection by Backscattering	3
2.2	Spectrometer Layout	5
2.3	Measuring Spectra	7
2.4	Instrument Characteristics	7
3	Applications	8
3.1	Hyperfine Splitting	8
3.2	Molecular Rotation and Quantum Tunneling	9
4	Preparatory Exercises	11
5	Experiment Procedure	12
5.1	The experiment itself	12
5.2	Raw data reduction	12
5.3	Data evaluation	12
	Contact	14

1 Introduction

Neutron *backscattering spectrometers* are used to measure *inelastic scattering* with very high *energy resolution*. What does this mean?

In inelastic scattering, scattering intensity is measured as function of the energy exchanged between the scattered neutron and the sample. As in other areas of physics, a data set of the form intensity-versus-energy is called a *spectrum*. An instrument that resolves inelastic scattering is therefore called a *spectrometer*.

While elastic scattering experiments yield information about *structure* or *texture* of a sample, inelastic scattering is used to investigate its *dynamics*. Specifically, inelastic neutron scattering yields information about the thermal motion of atomic nuclei.

The most common instrument for inelastic neutron scattering is the triple-axis spectrometer. It is routinely used to measure phonon and magnon dispersions, with energy exchanges of the order of meV. In contrast, the *high resolution* of a backscattering spectrometer allows to resolve very *small energy shifts* of the order of μeV . By the time-energy uncertainty relation, small energy means long times. Hence, backscattering addresses relatively *slow* nuclear motion — much slower than the lattice vibrations typically seen in triple-axis spectrometry.

What processes take place on the energy or time scale made accessible by neutron backscattering? For instance the following:

- hyperfine splitting of nuclear spin orientations in a magnetic field,
- rotations or hindered reorientations of molecules or molecular side groups,
- quantum tunneling,
- hydrogen diffusion in solids,
- relaxation (molecular rearrangements) in viscous liquids,
- innermolecular rearrangements in polymers.

During your lab course day, you will use the backscattering spectrometer SPHERES (SPectrometer for High Energy RESolution) to study one example of these applications.

2 Spectrometer Physics

2.1 Energy Selection by Backscattering

In crystal spectrometers, neutron energies are selected by Bragg reflection from crystals, according to the *Bragg condition*

$$n\lambda_n = 2d_{hkl} \sin \Theta \quad (1)$$

where d_{hkl} is the distance of lattice planes $[hkl]$, and Θ is the glancing angle of reflection from these planes. The index n indicates that along with a fundamental wavelength λ_1 , integer fractions $\lambda_n = \lambda_1/n$ are transmitted as well. To suppress these unwanted higher orders, experimental setups include either a mechanical neutron velocity selector (Fig. 1), or a beryllium filter.

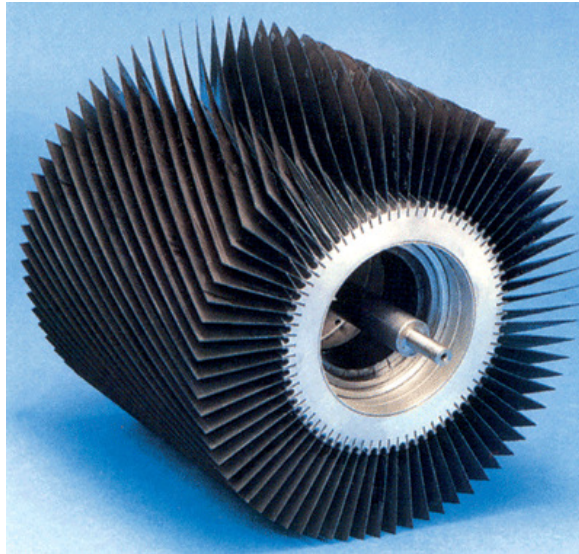


Fig. 1: Rotor of a mechanical neutron velocity selector. The blades are coated with neutron absorbing material. In SPHERES, such a selector is used as a pre-monochromator that reduces the incoming white spectrum to about $\pm 6\%$. © Astrium GmbH.

In practice, the parameters d and Θ on the right-hand side of Eq. (1) are not sharp: Imperfections of the crystal lead to a distribution of lattice constants, characterized by a width δd . And similarly, imperfections of the neutron optics (inevitable because the incoming beam, the sample, and the detector all have finite size) lead to a distribution of reflection angles, characterized by a width $\delta\Theta$. By differentiating the Bragg equation (1), one obtains the relative width of the wavelength distribution reflected by a crystal monochromator:

$$\frac{\delta\lambda}{\lambda} = \frac{\delta d}{d} + \cot \Theta \delta\Theta. \quad (2)$$

In usual crystal spectrometers, the second term is the dominant one. However, by choosing $\Theta = 90^\circ$, the prefactor $\cot \Theta$ can be sent to zero. This is the fundamental idea of the backscattering spectrometer. If a monochromator crystal is used in backscattering geometry, with $\Theta \simeq 90^\circ$, then the reflected wavelength distribution is in first order insensitive to the geometric imperfection $\delta\Theta$; it depends only on the crystal imperfection δd and on a second-order $(\delta\Theta)^2$ term.

The monochromator of SPHERES is made of silicon crystals in (111) orientation (Fig. 2). The backscattered wavelength is $\lambda = 2d_{111} = 6.27 \text{ \AA}$, corresponding to a neutron energy of 2.08 meV. The crystals are cut from wafers produced by the semiconductor industry. They are perfectly monocrystalline, so that their intrinsic resolution¹ of $\delta d/d \simeq 10^{-6}$ is actually too good because it does not match the spectrometer's second-order geometric imperfection $(\delta\Theta)^2 \lesssim 10^{-4}$. As a remedy, the crystals are glued to a spherical support so that the resulting strain induces a lattice constant gradient of the order $\delta d/d \simeq 10^{-4}$.

¹ In perfect crystals, the intrinsic resolution $\delta d/d$ is limited by *primary extinction*: Say, each crystalline layer has a reflectivity of about 10^{-6} . Then only about 10^6 layers contribute to the Bragg reflection. This limits $\delta\lambda/\lambda$ to about 10^{-6} .

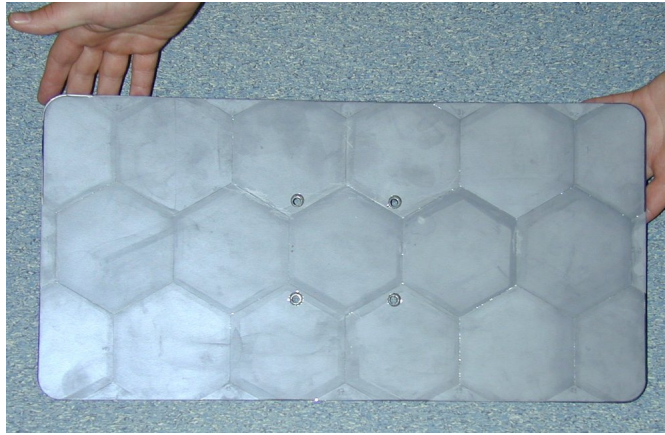


Fig. 2: The monochromator of SPHERES consists of hexagonal Si(111) wafers of $750\ \mu\text{m}$ thickness, glued onto a spherical support made of carbon fiber.

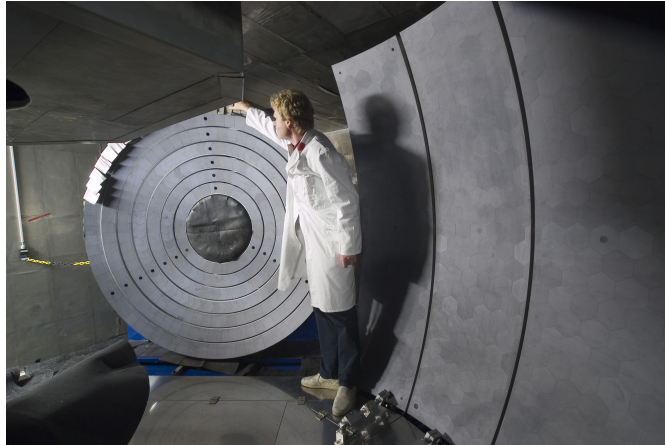


Fig. 3: The analyzers of SPHERES are made of the same Si(111) as the monochromator. For small scattering angles, they are shaped as rings; for large scattering angles, they are approximately rectangular sections of a sphere.

2.2 Spectrometer Layout

In a crystal spectrometer, a *monochromator* is used to send a neutron beam with a narrow energy distribution $E_i \pm \delta E$ onto the sample. After the sample, a second monochromator, called *analyzer*, is used to select a narrow energy distribution $E_f \pm \delta E$ out of the scattered spectrum. In SPHERES, we actually have a huge array of analyzers (Fig. 3), covering a solid angle of about 2.5, which is 20% of 4π . These analyzers send energy-selected neutrons towards 16 different detectors, depending on the scattering angle ϑ .

Fig. 4 shows the complete layout of SPHERES. The incoming beam is pre-monochromatized by a mechanical velocity selector. Then, it is transported by a focussing neutron guide into the instrument housing where it hits a rotating chopper. The chopper rotor (Fig. 5) carries mosaic crystals made of pyrolytic graphite on half of its circumference. When the incoming neutrons hit

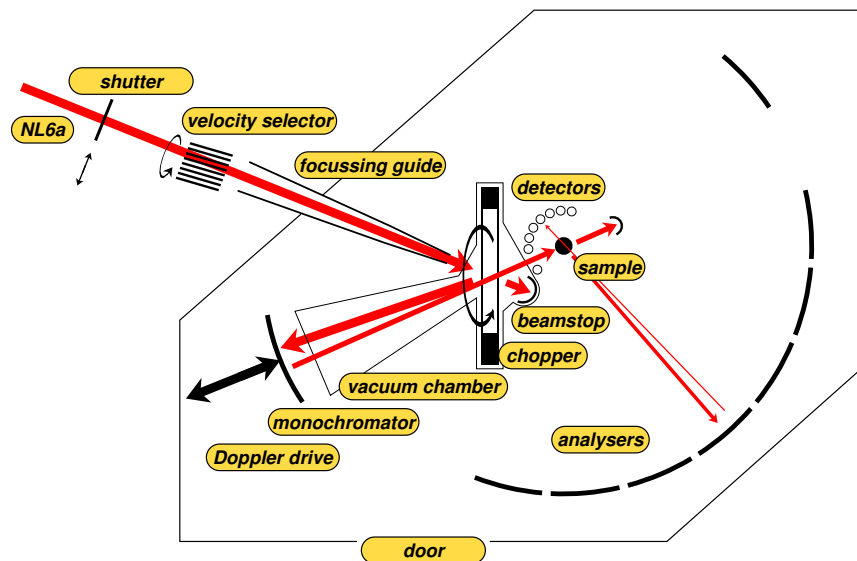


Fig. 4: Layout of the Jülich backscattering spectrometer SPHERES at FRM II.



Fig. 5: Schematic front view of the chopper rotor of SPHERES. The red bands indicate the mosaic crystals that deflect the incident beam towards the monochromator.

these crystals, they undergo a Bragg reflection towards the monochromator.² Otherwise, they are transmitted towards a beamstop.

The backscattering monochromator selects a neutron band $E_i \pm \delta E$ as described above. Neutrons within this band are sent back towards the chopper. When they reach the chopper, the rotor has turned by 60° : the mosaic crystals have moved out of the way; the neutrons coming from the monochromator are transmitted towards the sample.

The sample scatters neutrons into 4π . About 20% of this is covered by analyzers. If a scattered neutron hits an analyzer and fulfills the backscattering Bragg condition, it is sent back towards the sample. It traverses the sample³ and reaches a detector. To discriminate energy-selected neutrons from neutrons that are directly scattered from the sample into a detector, the time of arrival is put in relation to the chopper phase.

² As a side effect, the Bragg deflection by rotating mosaic crystals achieves a favorable *phase-space transform* (PST): the incoming wavevector distribution is spread in angle, but compressed in modulus. This results in a higher spectral flux in the acceptance range of the monochromator.

³ Of course not all neutrons are transmitted: some are lost, some are scattered into a wrong detector. This inaccuracy is inevitable in neutron backscattering. We strive to keep it small by using rather thin samples with typical transmissions of 90% to 95%.

While the primary spectrometer (everything before the sample) is mainly in vacuum, the secondary spectrometer is not. To minimize neutron losses in the secondary spectrometer, the entire instrument housing can be flooded with argon. For the labcourse, we preferentially remove the argon so that participants can accede the housing. However, since refilling takes at least one full day, time constraints may prevent us from doing so. In this case, a video will be shown to present the interior of the spectrometer.

2.3 Measuring Spectra

So far we have introduced a static arrangement with fixed energies $E_i = E_f$. Such an arrangement is actually used to measure the fraction of elastic versus total scattering, called the *Debye-Waller factor* for coherent scattering and the *Lamb-Mössbauer factor* for incoherent scattering. More often, however, one wants to measure full spectra $S(Q, \omega)$. Therefore, one must find a way to modify the energy transfer

$$\hbar\omega = E_i - E_f. \quad (3)$$

This can be done using the *Doppler effect*: The monochromator is mounted on a linear drive that performs a cyclic motion. In the monochromator's rest frame, the backscattered energy is always the value $E_0 = 2.08$ meV given by the lattice constant of Si(111). Depending on the monochromator's velocity v , the value in the laboratory frame is

$$E_i(v) = \frac{m_n}{2} (v_0 + v)^2 \quad (4)$$

where $v_0 = 631$ m/s is the neutron velocity at $E_0 = m_n/2 v_0^2$. The Doppler drive of SPHERES has a linear amplitude of ± 75 mm and achieves a velocity amplitude of ± 4.7 m/s, resulting in an energy range

$$-30.7 \mu\text{eV} < \hbar\omega < 30.9 \mu\text{eV}. \quad (5)$$

This is called the *dynamic range* of the spectrometer.

When a scattered neutron is detected, its time of flight is traced back to the moment when it has been backscattered by the monochromator. From the recorded trace of the linear drive, the monochromator velocity at that moment is inferred, ω is computed from (4) and (3), and the corresponding histogram channel is incremented. To determine $S(Q, \omega)$, one needs to normalize to the time spent in channel ω . This normalization is routinely done by the instrument's raw-data reduction program SLAW.

2.4 Instrument Characteristics

The performance of a spectrometer can be characterized by its *resolution function*. To obtain the resolution function, one measures the spectrum of a purely elastic scatterer. Fig. 6 shows the result of a resolution measurement from a user experiment on SPHERES. Note the logarithmic intensity scale.

Conventionally, the resolution of an instrument is characterized by the *full width at half maximum* (FWHM). For SPHERES, a typical value is $0.65 \mu\text{eV}$. Note however that the FWHM is

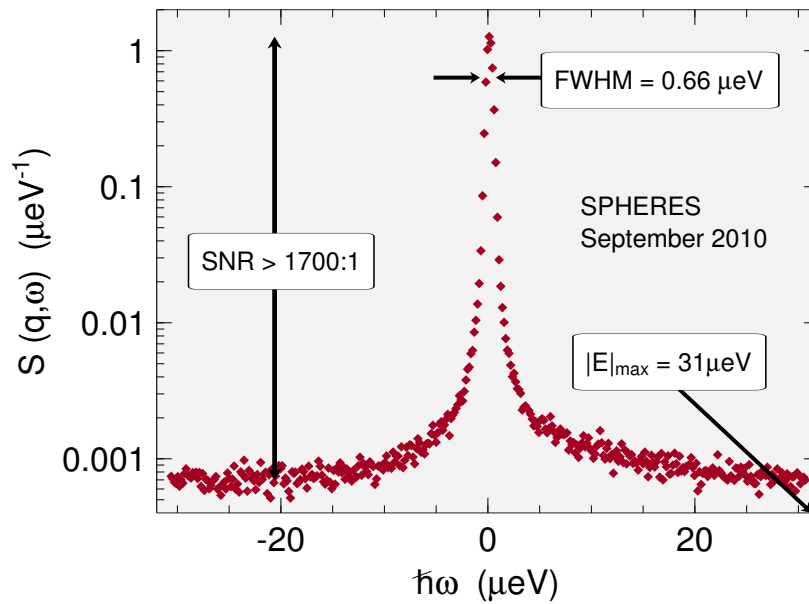


Fig. 6: Resolution function of SPHERES, measured on a user provided sample at a low temperature where the scattering is purely elastic.

not the full story: the quality of an instrument also depends on the *shape* of the resolution functions, especially of the deep wings. The resolution of SPHERES is slightly asymmetric. This is related to the $(\delta\Theta)^2$ term in the wavelength spread of a backscattering analyzer: all deviations from the perfect $\Theta = 90^\circ$ geometry lead to the transmission of longer wavelengths, never of shorter ones.

Another important figure of merit is the *signal-to-noise ratio* (SNR). It depends strongly on the ratio of scattering to absorption cross sections and on the thickness and geometry of the sample. With argon filling, the best value obtained in user experiments has been 1700:1; without argon, 1200:1. On the other hand, for strongly absorbing samples it is sometimes less than 100:1.

3 Applications

In the following, two different applications of neutron backscattering are explained: hyperfine splitting in a magnetic material, and methyl group tunneling.

3.1 Hyperfine Splitting

The measurement of hyperfine splitting has been historically the first application of neutron backscattering,⁴ and to this day, it is the conceptually simplest one.

Since the neutron has spin $S = 1/2$, its magnetic quantum number can take the values $S_z = \pm 1/2$. In a scattering event, this quantum number can change. In more pictorial words: when a

⁴ A. Heidemann, Z. Phys. 238, 208 (1970).

neutron is scattered, it may or may not undergo a *spin flip*.

As angular momentum is conserved, a change of S_z must be accompanied by an opposite change of the magnetic quantum number I_z of the nucleus by which the neutron is scattered, $\Delta I_z = -\Delta S_z$. Therefore, spin-flip scattering is only possible if the sample contains nuclei with nonzero spin I .

Nuclei with nonzero spin quantum number I possess a magnetic moment

$$\mu = Ig\mu_N \quad (6)$$

with the nuclear magneton

$$\mu_N = \frac{e\hbar}{2m_p} = 3.153 \cdot 10^{-8} \text{ eV/T}. \quad (7)$$

The g factor is different for each nucleus.⁵

A local magnetic field B leads to a splitting of energy levels,

$$E = I_z g \mu_N B, \quad (8)$$

called *hyperfine splitting*. Consequently spin-flip scattering is accompanied by an energy exchange $\Delta E = \pm g \mu_N B$. By measuring the neutron energy gain or loss $\pm \Delta E$, one can accurately determine the local field B in ferromagnetic or antiferromagnetic materials.

3.2 Molecular Rotation and Quantum Tunneling

Rotational motion of molecules or molecular side groups is one of the most important applications of neutron backscattering. Here, we specialize on the rotation of methyl (CH_3) groups. We consider these groups as stiff, with fixed⁶ CH bond length 1.097 Å and HCH angle 106.5°.

The only degree of freedom is then a rotation around the RC bond that connects the methyl group to the remainder R of the molecule. This RC bond coincides with the symmetry axis of the CH_3 group. The rotational motion can therefore be described by a wave function ψ that depends on one single coordinate, the rotation angle ϕ .

The Schrödinger equation is

$$\left\{ B \frac{\partial^2}{\partial \phi^2} - V(\phi) + E \right\} \psi(\phi) = 0. \quad (9)$$

For free rotation ($V = 0$), solutions that possess the requested periodicity are sine and cosine functions of argument $J\phi$, with integer J . Accordingly, the energy levels are $E = BJ^2$.

Given the value $B = 670 \text{ } \mu\text{eV}$, it is obvious that free rotor excitations occur only far outside the dynamic range of neutron backscattering. Conversely, if we observe an inelastic signal from methyl groups on a backscattering spectrometer, then we must conclude that $V \neq 0$: the

⁵ Tabulation: <http://ie.lbl.gov/toipdf/mometbl.pdf>.

⁶ Ignoring the variations of empirical values, which are of the order of $\pm 0.004 \text{ } \text{Å}$ and $\pm 1.5^\circ$.

methyl group rotation is *hindered* by a rotational potential. This potential can be caused by the remainder R of the molecule as well as by neighbouring molecules.

Due to the symmetry of the CH₃ group, the Fourier expansion of $V(\phi)$ contains only sine and cosine functions with argument $3m\phi$, with integer m . In most applications, it is sufficient to retain only one term,

$$V(\phi) \doteq V_3 \cos(3\phi). \quad (10)$$

The strength of the potential can then be expressed by the dimensionless number V_3/B . In the following we specialize to the case of a *strong potential*, $V_3/B \gg 10$, which is by far the most frequent one.

In a strong potential of form (10), the CH₃ group has three preferential orientations, separated by potential walls. The motion of the CH₃ group consists mainly of small excursions from the preferred orientations, called *librations*. Essentially, they are harmonic vibrations.

At low temperatures, almost exclusively the vibrational ground state is occupied. Yet reorientational motion beyond librations is possible by means of quantum mechanical tunneling: the wave functions of the three localised *pocket states* ψ_m ($m = 1, 2, 3$) have nonzero overlap. Therefore, the ground state is a linear combination of pocket states.⁷ Periodicity and threefold symmetry allow three such combinations: a plain additive one

$$\psi_1 + \psi_2 + \psi_3, \quad (11)$$

and two superpositions with phase rotations

$$\psi_1 + e^{\pm i2\pi/3}\psi_2 + e^{\pm i4\pi/3}\psi_3. \quad (12)$$

In the language of group theory, state (11) has symmetry A , the degenerate states (12) are labelled E^a, E^b . It is found that A is the ground state. The *tunneling splitting* $\hbar\omega_t$ between the states A and E is determined by the overlap integral $\langle \psi_m | V | \psi_n \rangle$ ($m \neq n$). It depends exponentially on the height of the potential wall. Provided it falls into the dynamic range of neutron scattering, it leads to a pair of inelastic lines at $\pm \hbar\omega_t$.

With rising temperatures, the occupancy of excited vibrational levels increase. This facilitates transitions between A and E sublevels and results in a decrease of $\hbar\omega_t$ and a broadening of the inelastic lines.

Upon further temperature increase, thermal motion of neighbouring molecules causes so strong potential fluctuations that the picture of quantum tunneling is no longer applicable. Instead, the motion between different pocket states can be described as *stochastic jump diffusion*.

Let $p_m(t)$ be the probability of being in pocket state m ($m = 1, 2, 3$). Assume that jumps between the three main orientations occur with a constant rate τ^{-1} . Then, the p_m obey rate equations

$$\frac{d}{dt}p_m(t) = \frac{1}{\tau} \left\{ -p_m + \sum_{n \neq m} \frac{1}{2}p_n \right\}. \quad (13)$$

⁷ This is an extremely simplified outline of the theory. In a serious treatment, to get all symmetry requirements right, one must also take into account the nuclear spins of the H atoms. See W. Press, *Single-Particle Rotations in Molecular Crystals*, Springer: Berlin 1981.

The stationary equilibrium solution is just $p_m = 1/3$ for all m . When perturbed, the system relaxes into equilibrium with a time dependence of $\exp(-t/\tilde{\tau})$. Explicit solution of the linear differential equation system (13) yields $\tilde{\tau} = 2\tau/3$.

According to a fundamental theorem of statistical mechanics (the *fluctuation dissipation theorem*), the relaxation by which a slightly perturbed system returns *into* equilibrium has the same time dependence as the pair correlation function *in* equilibrium. Therefore, we can employ the solution of (13) to write down the self-correlation function of the protons that constitute our methyl group. Fourier transform yields then the incoherent scattering function

$$S(q, \omega) = a(q)\delta(\omega) + b(q)\frac{\Gamma}{\omega^2 + \Gamma^2}. \quad (14)$$

The first term describes elastic scattering. The second term, the Fourier transform of the exponential $\exp(-t/\tilde{\tau})$, is a Lorentzian with linewidth $\Gamma = \tilde{\tau}^{-1}$; such *broadening* of the elastic line is often called *quasielastic*.

4 Preparatory Exercises

1. Relate the relative wavelength spread $\delta\lambda/\lambda$ to the relative energy spread $\delta E/E$.
2. In SPHERES, useable detectors are located at scattering angles 2θ ranging from 12.5° to 134° . Calculate the corresponding wavenumbers in \AA^{-1} . Recommendation: use the following constants in *atomic units*: $\hbar c = 1973 \text{ eV}\text{\AA}$ and $m_n c^2 = 940 \text{ MeV}$.
3. Convert dynamic range and resolution of SPHERES into GHz. To make contact with optical spectroscopy, you might also wish to convert into cm^{-1} .
4. Empirically, it is found that the centre of the resolution function can be fitted by a Gaussian $a \exp(-E^2/2/\sigma^2)$. Derive an expression that relates the Gaussian standard deviation σ to the FWHM.
5. Note that the above mentioned fit applies only to the very centre of the resolution function. How does a Gaussian look like on the lin-log representation of Fig. 6? And a Lorentzian?
6. In SPHERES, the distance sample-analyzer is 2 m. Calculate the time neutrons need for a round trip sample-analyzer-sample, and deduce the rotation frequency of the chopper.
7. Assume that the monochromator motion is perfectly sinusoidal. Sketch how the measuring time per energy channel varies with $\hbar\omega$.
8. Draw a sketch of the expected backscattering spectrum $S(q, \omega)$ of a ferromagnetic material with $I \neq 0$.
9. Assume a hyperfine splitting of $\Delta E = 2 \text{ }\mu\text{eV}$. To which temperature do you have to cool the sample to observe a 10% difference between the probabilities of energy gain and energy loss scattering?
10. How do you expect ΔE to evolve when the sample is heated towards the Curie or Néel temperature?

11. Calculate the moment of inertia, $I = \sum mr_{\perp}^2$, of a methyl group. Verify that the *rotational constant* $B = \hbar^2/(2I)$ has a value of about 670 μeV .
12. Expand $V(\phi)$ around a potential minimum, and compare the resulting Schrödinger equation with that of a harmonic oscillator. Show that the splitting of oscillator levels is of the order of meV.
13. Draw a coordinate system energy-versus-angle. Sketch $V(\phi)$, the harmonic approximation, the ground state's $\psi(\phi)$, and the lowest oscillator energy levels. What does that imply for the validity of the oscillator approximation?
14. Sketch the expected spectra for different temperatures.

5 Experiment Procedure

5.1 The experiment itself

After an initial discussion, methyl group tunneling will be studied. For a given chemical composition, the group computes the sample thickness that yields 90% transmission. Depending on the group's interest, a sample is prepared, or a standard sample is used. The tutor shows how to insert the sample in the instrument's cryostat. Using the instrument's graphical user interface, starting a measurement is rather trivial. Log entries are written to the instrument log wiki.

5.2 Raw data reduction

The program SLAW is used to convert raw neutron counts into $S(Q, \omega)$. It is parametrized by a script, called `slawfile`. The tutor provides a sample script, which is then modified to convert the results of the current experiment.

SLAW can save $S(Q, \omega)$ in a variety of output formats. Most relevant are plain tabular formats `recttab` and `spectab`, and a self-documenting format `y08` required by our standard data-analysis software FRIDA.

5.3 Data evaluation

In a first approach, labcourse participants should analyse plain tabular data using whatever all-purpose data-analysis software they are used to.

1. Plot a representative selection (choose a few Q) of measured spectra.
2. Determine the FWHM of the elastic line, and of the inelastic lines if there are any.
3. Try to fit these lines with a Gaussian, with a Lorentzian, with a squared Lorentzian.
4. Summarize the temperature dependence of the spectra.

For a more quantitative analysis, it is necessary to convolute a theoretical model with a measured resolution function. This can be done with the data-analysis package FRIDA. For a tutorial, refer to the SPHERES wiki.⁸

⁸ Follow the link at http://www.jcns.info/jcns_spheres.

Contact

SPHERES

Phone: 089/289-14875

Web: http://www.jcns.info/jcns_spheres/

Joachim Wuttke

JCNS at FRM II, Forschungszentrum Jülich GmbH

Phone: 089/289-10715

e-Mail: j.wuttke@fz-juelich.de

Gerald J. Schneider

Phone: 089/289-10718

e-Mail: g.j.schneider@fz-juelich.de